Published for SISSA by Springer

Received: *May 17, 2015*
Revised: *August 21, 2015*
Accepted: *September 1, 2015*
Published: *September 22, 2015*

Majorana dark matter through a narrow Higgs portal

M. Dutra, C.A. de S. Pires and P.S. Rodrigues da Silva

Universidade Federal da Paraíba,
João Pessoa-PB, Brasil

E-mail: mdutra@fisica.ufpb.br, cpires@fisica.ufpb.br, psilva@fisica.ufpb.br

Abstract: We update the parameter space of a singlet Majorana fermion dark matter model, in which the standard particles interact with the dark sector through the mixing of a singlet scalar and the Higgs boson. In this model both the dark matter and the singlet scalar carry lepton number, the latter being a bilepton. The stability of the Majorana fermion is achieved by a supposed Z_2 symmetry. The lepton number symmetry breaking scale, driven by the singlet scalar, is constrained to be within hundreds to thousands of GeV, so as to give a sufficiently abundant Majorana fermion. Relic density, direct detection and invisible Higgs decay are considered in a complementary way, as we contrast our parameter space with the Planck, LUX and LHC bounds. The impacts of the future Higgs self-coupling measurements and of XENON1T detector are also discussed. We find a "narrow" Higgs portal in the sense that large deviations from the standard scalar sector (large mixing and low lepton breaking scale) are very restricted by Higgs data global fit. We perform a systematic study of the allowed parameter space, favored by scalar resonances and degeneracy. One important phenomenological signature of this model is the correlation between the discoveries of a dark matter and a singlet scalar particles. Very light singlet scalars were found disfavored by direct detection, interestingly implying that the Majoron present in our spectrum can hardly be a dark radiation candidate if our scenario addresses the DM issue. This model is very predictive and in the next few years should be completely tested by the experiments.

Keywords: Higgs Physics, Beyond Standard Model, Cosmology of Theories beyond the SM, Global Symmetries

ArXiv ePrint: 1504.07222

doi:10.1007/JHEP09(2015)147

JHEP09(2015)147

Contents

1 Introduction

Since almost a century ago, a huge amount of evidences has been accumulated through astrophysics observations [1–6], indicating that the majority of matter in the Universe is of unknown origin. Such observations, however, refer specifically to the gravitational response of ordinary (or baryonic) matter to this so called Dark Matter (DM), scarcely showing other properties it should comply with, except that it has to be effectively electrically neutral,[1] non-baryonic, cosmologically stable and cold at recombination. These are important clues in order to start building a model to describe the DM. Particle Physics is strongly appealing in offering a DM candidate, since many motivating extensions of the standard model of electroweak interactions (SM) possess new fields and symmetries, which could suitably provide one (or more) stable particle(s) in their spectrum.

The first observational requirement that a DM model has to fulfill is a set of interactions that can account for the relic density inferred from the power spectrum of the cosmic microwave background radiation. As it says nothing about the particle nature of the DM candidate, such as its mass, spin or charges, we have to count on the possibility of detecting a signal from a DM particle and gathering more information in order to put this particle under siege. Such a signal should be identified in underground detectors (direct detection search), in satellites or ground-based telescopes (indirect detection search) as well as in colliders or accelerators (collider search). There are many experiments searching for DM candidates, especially the weakly interacting massive particles (WIMPs). Currently, no

[1] Milli-charged DM candidates exist in the literature which are perfectly acceptable though [7–9].

JHEP09(2015)147

unambiguous positive DM signal was announced by the experiments, but limits were put on its scattering cross-section off nucleon and production rate.

Any viable particle physics model that addresses the DM issue must comply with these bounds and may be constructed in a top-down or a bottom-up way. The top-down models intend to explain open particle physics problems in a fundamental way while having a DM candidate, such as supersymmetric and extra-dimension models. The bottom-up models intend to minimally explain the DM physics, with just a few free parameters and strong predictions, and are more easily ruled out by the experiments. This strategy, that we will adopt here, allows us to identify which initial hypothesis can be modified in order to agree with the experimental limits.

Models in which the interaction between DM and standard particles is realized through scalar exchanges, the Higgs portal, are phenomenologically interesting since the discovery of the Higgs-like scalar at the LHC [10, 11]. As its couplings and branching ratios are being measured, the Higgs physics can constrain the parameter space of such DM models. Here, we focus on the fermionic DM in a minimal Higgs portal model. Fermionic DM particles may be Majorana or Dirac particles, differing in their relic abundance which is twice larger for Dirac fermions, to account for the fact that there are two distinct particles annihilating. Also, the scattering cross-section off nucleon of a Majorana fermion is twice larger relative to a Dirac fermion. In many respects there is no significant difference between Dirac and Majorana fermion DM candidates though, as pointed out in previous works [12–16].

Singlet Dirac DM candidates were vastly explored in the context of Higgs portal models after the Higgs discovery [17–21]. It is known that a lighter than 100 GeV Dirac DM is excluded by relic, direct detection and collider constraints, except at the resonance region [22, 23]. Although less considered, a Majorana DM in renormalizable Higgs portal models were also pointed out as viable DM candidates [14, 15, 24].

The implications of the 125 GeV scalar for Higgs Portal DM models were studied in a model independent way in ref. [25], considering generic scalar, Majorana fermion and vector DM candidates in the effective field theory (EFT) framework. EFT models with Majorana DM were also considered in [13, 14, 26]. Within EFT approach, the CP-conserving Higgs portal of a fermionic DM is excluded by direct detection search for the DM mass range of 60 GeV–2 TeV. Nevertheless, it remains viable if we consider UV completions such as a resonant or an indirect Higgs portal [14]. Since we do not know the mass scales of the possible intermediate particles, we can not know if an EFT approach is valid in the context of Higgs Portal DM models. Indeed, even though renormalizable models must agree with EFT models in the limit of heavy mediators, some degrees of freedom concerning the mediator phenomenology are only appreciable in concrete models.

In this work, we consider a sterile Majorana neutral fermion as DM candidate in a renormalizable CP-conserving Higgs portal model [27], under the light of the recent experimental limits. We suppose the existence of a discrete Z_2 symmetry responsible for the Majorana fermion stability, that is expected as a remnant of some spontaneously broken gauge symmetry at a high scale not relevant for the low energy physics. The mediator between the Majorana fermion and the standard particles is a complex singlet scalar that develops a nonzero vacuum expectation value (vev), thus breaking lepton number symmetry.

JHEP09(2015)147

This work is the first consideration of the LUX impact on the parameter space of a minimal concrete Majorana DM Higgs portal model. We also consider the XENON1T future sensitivity, the invisible Higgs decay (IHD) constraint and comment how the extension of the scalar sector alters the Higgs self-couplings, showing that their future measurements will put important bounds on our parameter space.

This work is organized as follows: in the next section we will present our model. In section 3 we compute the relic density and scattering cross section off nucleon for the Majorana fermion, in order to constrain our parameter space and discuss how the free parameters influence these observables. We also comment the impact of the future measurements of the Higgs self-couplings on the free parameters and the possibility of having a dark radiation candidate in our scenario. Our main results are presented in section 4, where we update the parameter space taking into account the IHD and LUX bounds and the XENON1T future sensitivity, and in section 5 we give our conclusions. In appendix A we show the amplitudes for the processes that set the relic density of the Majorana fermion.

2 The model

The model we consider here consists in a singlet Majorana right-handed neutral fermion, N_R, as a DM candidate, whose interaction with the SM particles is through a Higgs portal opened by a singlet complex scalar, σ, that mix to the SM Higgs doublet, ϕ. This Majorana fermion is sterile and stable, a requisite for a DM candidate, when non-trivially transforming under a Z_2 symmetry, which forbids it to mix to the light neutrinos and makes it interact only with the singlet scalar field.

We build our Lagrangian assuming lepton number conservation. Considering that N_R carries one unit of lepton number, no explicit mass term for it is present in the Lagrangian. Its mass is generated from an Yukawa term involving the σ field when it acquires a nonzero vev and breaks the lepton number symmetry. These assumptions reduce the number of free parameters in our model, in comparison with the Majorana fermion models we referenced.

The most general renormalizable Lagrangian to be added to the SM, under the above assumptions, is given by

$$\mathcal{L} \supset \mathcal{L}_{kin}(N_R, \sigma) - \lambda_N(\overline{N_R^c} N_R \sigma + \overline{N_R} N_R^c \sigma^*) - V(\phi, \sigma), \tag{2.1}$$

where $\mathcal{L}_{kin}(N_R, \sigma)$ is the kinetic term for the new singlet fields and the scalar potential is

$$\begin{aligned} V(\phi, \sigma) = \; & \mu_\phi^2 \phi^\dagger \phi + \lambda_\phi (\phi^\dagger \phi)^2 + \mu_\sigma^2 \sigma^* \sigma + \lambda_\sigma (\sigma^* \sigma)^2 \\ & + \lambda_{\phi\sigma} (\phi^\dagger \phi)(\sigma^* \sigma). \end{aligned} \tag{2.2}$$

After spontaneous breaking of electroweak and lepton number symmetries, when $\langle \phi^0 \rangle \equiv v_\phi/\sqrt{2}$ and $\langle \sigma \rangle \equiv v_\sigma/\sqrt{2}$, the above potential leads to the minimum conditions

$$v_\phi^2 = -\frac{\mu_\phi^2 + \lambda_{\phi\sigma} \langle \sigma^2 \rangle_0}{\lambda_\phi} \tag{2.3}$$

and

$$v_\sigma^2 = -\frac{\mu_\sigma^2 + \lambda_{\phi\sigma} \langle \phi^2 \rangle_0}{\lambda_\sigma}\,. \tag{2.4}$$

JHEP09(2015)147

The physical spectrum is then obtained by shifting the scalar fields to the physical fields, that can be written in the unitary gauge as,

$$\phi = \frac{1}{\sqrt{2}} \begin{pmatrix} 0 \\ v_\phi + R_\phi \end{pmatrix} \tag{2.5}$$

and

$$\sigma = \frac{v_\sigma + R_\sigma + iJ}{\sqrt{2}}\,. \tag{2.6}$$

Observe that the breaking of lepton number symmetry implies the existence of a Majoron in the spectrum, J, which was shown to be a phenomenologically safe Goldstone boson [27]. The mass matrix of the scalar fields is given by

$$M^2 = \begin{pmatrix} 2\lambda_\phi v_\phi^2 & \lambda_{\phi\sigma} v_\phi v_\sigma \\ \lambda_{\phi\sigma} v_\phi v_\sigma & 2\lambda_\sigma v_\sigma^2 \end{pmatrix}. \tag{2.7}$$

By diagonalizing the mass matrix with the orthogonal matrix

$$\begin{pmatrix} \cos\alpha & -\sin\alpha \\ \sin\alpha & \cos\alpha \end{pmatrix}, \tag{2.8}$$

(hereafter we denote $\cos\alpha$ and $\sin\alpha$ by c_α and s_α) we have the physical states given by

$$\begin{aligned} H &= c_\alpha R_\phi + s_\alpha R_\sigma \\ S &= -s_\alpha R_\phi + c_\alpha R_\sigma, \end{aligned} \tag{2.9}$$

provided that the mixing angle α is defined as

$$\tan 2\alpha \equiv \frac{\lambda_{\phi\sigma} v_\phi v_\sigma}{\lambda_\phi v_\phi^2 - \lambda_\sigma v_\sigma^2}. \tag{2.10}$$

Since the discovery of a scalar resonance in the CMS and ATLAS experiments at LHC [10, 11], with mass around 125 GeV, and whose interactions indicate it is most probably the SM Higgs boson, we can be sure that this scalar cannot be a singlet under $\mathrm{SU}(2)_L$. In our case, it has to come from the doublet-like scalar, R_ϕ, implying that the mixing angle in eq. (2.9) has to be small. This is further corroborated by the null search results for a lighter than 125 GeV scalar, once the couplings of SM fields to the singlet scalar are suppressed by s_α. We then identify the mass eigenstates by

$$M_H^2 = 2(\lambda_\phi v_\phi^2 c_\alpha^2 + \lambda_\sigma v_\sigma^2 s_\alpha^2 + \lambda_{\phi\sigma} v_\phi v_\sigma s_\alpha^2 c_\alpha^2) \tag{2.11}$$

for the Higgs scalar and

$$M_S^2 = 2(\lambda_\sigma v_\sigma^2 c_\alpha^2 + \lambda_\phi v_\phi^2 s_\alpha^2 - \lambda_{\phi\sigma} v_\phi v_\sigma s_\alpha^2 c_\alpha^2) \tag{2.12}$$

for the singlet scalar.

JHEP09(2015)147

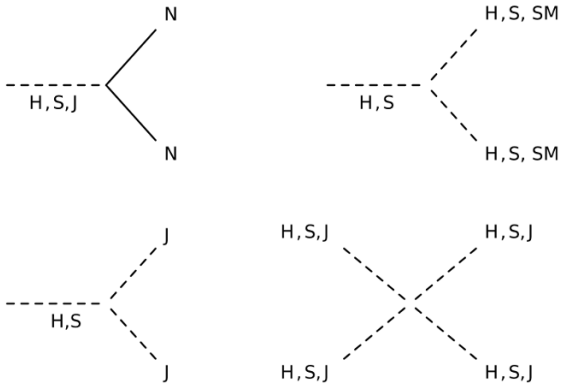

Figure 1. New interactions of the SM extension we are considering.

In terms of the mass eigenvalues, the mixing angle and the mixing coupling are determined by

$$\sin 2\alpha = \frac{2\lambda_{\phi\sigma} v_\phi v_\sigma}{M_H^2 - M_S^2} \qquad \lambda_{\phi\sigma} = s_\alpha c_\alpha \frac{M_H^2 - M_S^2}{v_\phi v_\sigma}. \tag{2.13}$$

As a consequence of the mixing (eq. (2.9)), all the standard couplings to the Higgs boson will be rescaled in our model by c_α. It allows us to probe this model at colliders, looking for deviations from the standard interactions with the Higgs boson. For further numerical convenience, we can solve the eqs. (2.11) and (2.12) for the quartic couplings, giving

$$\lambda_\phi = \frac{c_\alpha^2 M_H^2 + s_\alpha^2 M_S^2}{2v_\phi^2} \qquad \lambda_\sigma = \frac{c_\alpha^2 M_S^2 + s_\alpha^2 M_H^2}{2v_\sigma^2}. \tag{2.14}$$

The tree level stability of the scalar potential is guaranteed once $\lambda_\phi > 0$, $\lambda_\sigma > 0$ and $-2\sqrt{\lambda_\phi \lambda_\sigma} < \lambda_{\phi\sigma} < 2\sqrt{\lambda_\phi \lambda_\sigma}$, which we will use throughout this work.[2]

To complete the spectrum we write down the Majorana fermion mass after the spontaneous breaking of lepton number,

$$M_N = \sqrt{2}\lambda_N v_\sigma. \tag{2.15}$$

The non-standard interactions introduced by this extension of SM are presented in figure 1.

In summary, from the twelve free parameters, $\lambda_N, \mu_\phi^2, \mu_\sigma^2, \lambda_\phi, \lambda_\sigma, \lambda_{\phi\sigma}, M_N, M_S, M_H, v_\phi, v_\sigma$ and α, when we consider the six constraints, eqs. (2.3), (2.4), (2.10), (2.11), (2.12 and 2.15), and fix the Higgs mass in $M_H = 125\,\text{GeV}$ and the electroweak scale in $v_\phi = 246.22\,\text{GeV}$, we may choose to keep the remaining independent set of parameters as M_N, M_S, v_σ and α. In what follows, we discuss the role of each of them in the observables.

[2]The stability of a somewhat similar model at one loop level, where the scalar is real and the DM is a Dirac fermion, was considered in ref. [23] while, in ref. [20], the DM issue was also analyzed along with the possibility of a first order phase transition. This last feature not reproducible by our model.

JHEP09(2015)147

M_N (GeV)	M_S (GeV)	v_σ (GeV)	α
[1,2000]	[0.1,2000]	[100,2000]	[-0.5735,0.5735]

Table 1. Ranges for the free parameters used in our numerical scans.

3 Constraining the parameter space

Our parameter space is constrained by many requirements. First of all, the Majorana fermion must be sufficiently abundant in order to be a viable DM candidate. Here we use the latest results (2015) of the Planck satellite [28], in which the cold dark matter abundance is restricted to be $\Omega h^2 = 0.1199 \pm 0.0022$. Regarding the direct detection, we use the first results (2013) of the LUX experiment [29], with 118 kg of fiducial volume during the 85.3 live-day exposure (300 live-day is expected for the full-mission). This is the most sensitive upper limit on the WIMP spin independent (SI) scattering cross section off nucleon up to date ($\sim 7 \times 10^{-10}$ pb at a WIMP mass of 33 GeV). We also consider the XENON1T experiment [30], projected to operate with 1.1 ton of fiducial volume in 2 years live-time. An upper limit of $\sim 2 \times 10^{-11}$ pb at a WIMP mass of 50 GeV is expected for 2017. We computed the relic density and the scattering cross section off nucleon for the Majorana fermion, using the numerical package `micrOMEGAs` [31].

In order to carry out numerical scans on the parameter space, we randomly sampled all the free parameters in the ranges shown in table 1, always keeping $M_H = 125\,\text{GeV}$ and $v_\phi = 246.22\,\text{GeV}$. In ref. [32], we find that the unitarity and perturbativity bounds together require $M_N, M_S < 3\,\text{TeV}$ and $v_\sigma < 2.4\,\text{TeV}$.[3] Throughout this work, each point in the scans correspond to a set of free parameter values satisfying the following conditions:

- $|\alpha| < 0.5735$, to be consistent with the LHC bound for the mixing ($|cos(\alpha)| > 0.84$ [33]);
- $\lambda_\phi > 0$, $\lambda_\sigma > 0$ (automatic, see eq. (2.14)) and $-2\sqrt{\lambda_\phi \lambda_\sigma} < \lambda_{\phi\sigma} < 2\sqrt{\lambda_\phi \lambda_\sigma}$ for a potential bounded from below;
- Perturbativity: $\lambda_{\phi\sigma}, \lambda_\phi, \lambda_\sigma < 4\pi$.

It is instructive to emphasize that this parametrization allows us to consider the two possible scalar mass hierarchies: for a positive (negative) $\lambda_{\phi\sigma}$, $\alpha > 0$ ($\alpha < 0$) ensures that $M_S < M_H$ and $\alpha < 0$ ($\alpha > 0$) ensures that $M_S > M_H$, as we can see in figure 2. In this figure, we see the projection of all the parameter space (with the free parameters varying according to table 1) onto the ($\lambda_{\phi\sigma}$,α) plane.

An important feature of this Higgs Portal model is that the ongoing characterization of the discovered Higgs boson can provide valuable constraints on the free parameters. One example of this is the future measurement of the Higgs self-couplings [34–37]. The 3-Higgs

[3] Although these results are based on the assumption that the Majorana mass terms for fermionic DM are absent at tree level, we can naively assume they may be used in our case.

JHEP09(2015)147

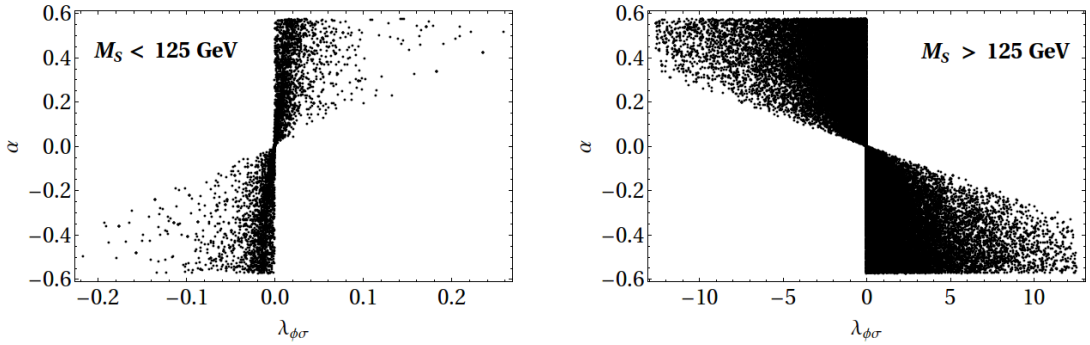

Figure 2. Projections of the parameter space onto the ($\lambda_{\phi\sigma}$,α) plane, for a lighter (left) and heavier (right) than Higgs singlet scalar. Note that the former case is possible only for a very weak mixing coupling.

and 4-Higgs self-couplings in our model are given by

$$\lambda_{HHH} = \frac{M_H^2}{2v_\phi}\left(c_\alpha^3 - s_\alpha^3 \frac{v_\phi}{v_\sigma}\right) \tag{3.1}$$

and

$$\lambda_{HHHH} = c_\alpha^4 \frac{\lambda_\phi}{4} + s_\alpha^4 \frac{\lambda_\sigma}{4} + s_\alpha^2 c_\alpha^2 \frac{\lambda_{\phi\sigma}}{4}. \tag{3.2}$$

In figure 3, we see the projections of the parameter space onto the (λ_{HHH}, α) (left) and (M_S, λ_{HHHH}) (right) planes. For the 3-Higgs self-coupling, we see that deviations from the SM value ($\lambda_{HHH} = 31.73\,\text{GeV}$) give us information about the intensity of the scalar mixing. Following [33], we see in the 3-Higgs self-coupling projection the bands corresponding to the future collider sensitivities: deviations from the SM predicted value of ±50% (TLEP500 / HL-LHC-min) are in blue, ±30% (TLEP240 / CEPC HL-LHC-max) in magenta, ±13% (ILC) in green and ±5% (hadron100TeV) in yellow. For the 4-Higgs self-coupling, we see that significant deviations from the SM value ($\lambda_{HHHH} = 0.032$) will be able to establish the scalar mass hierarchy in our scenario. With this picture in mind we can follow with the analysis of the DM constraints on the parameter space.

3.1 Relic density

In this work we are assuming thermal production of dark matter, thus the Majorana fermion relic density is determined by calculating the thermal averaged annihilation cross section for the processes shown in figure 4. The amplitudes for these processes are shown in appendix A.

As the dark matter in our scenario interacts by scalar exchanges, a characteristic behavior of the relic density is one sharply peaked region at $M_N \approx M_H/2 \approx 63\,\text{GeV}$, corresponding to the Higgs production and depending on the scalar mixing, and another one at $M_N \approx M_S/2$, corresponding to the singlet scalar production. As an asymptotic behavior, we expect a gradual decrease in the relic density, as more channels become kinematically open for heavier Majorana fermions.

In figure 5, we show the projection of the parameter space onto the $(M_N, \Omega h^2)$ plane. Our parameter scan shows that there is no set of free parameters allowing for sufficiently

JHEP09(2015)147

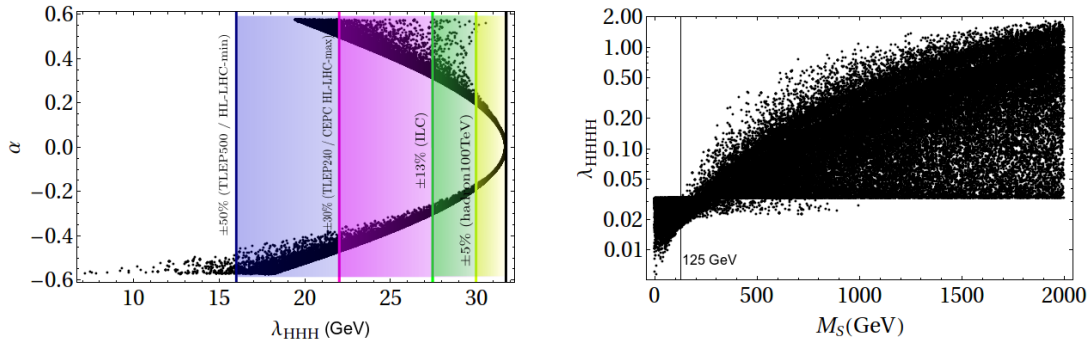

Figure 3. 3-Higgs (left) and 4-Higgs (right) self-couplings as functions of α and M_S, respectively. Note that deviations from the SM values give us information about the intensity of the scalar mixing as well as the scalar mass hierarchy. In the left panel, the colored bands are prospect deviations from the SM predicted value (black line) [33].

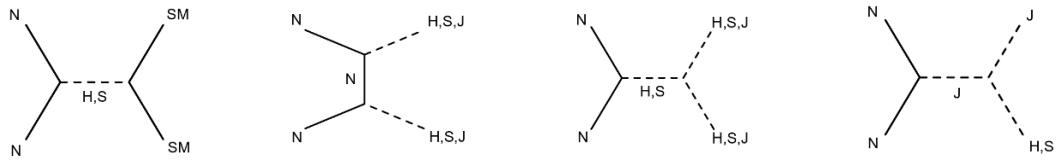

Figure 4. Annihilation channels relevant for the Majorana fermion relic density. See appendix A for the analytic expressions of their amplitudes.

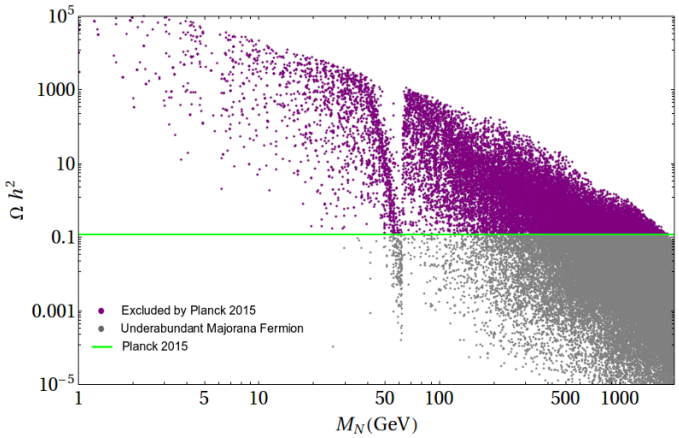

Figure 5. Relic density as a function of the Majorana fermion mass. The green interval represents the Planck bound on the relic density. The purple points overclose the Universe and will not be considered in our analysis. The gray points indicate regions of our parameter space in which the Majorana fermion is not sufficient to account for the total DM content of the Universe.

JHEP09(2015)147

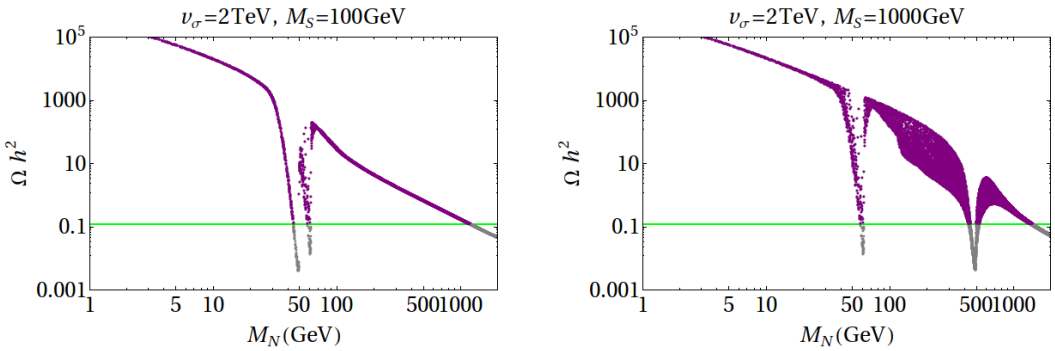

Figure 6. Singlet scalar resonances, for all values of the mixing angle. Notice that the Planck-allowed points (which intercept the green line) are always near the scalar resonances and where the abundance curve falls down. It is a characteristic behavior of this model, as we will see in more detail in what follows. Same color code of figure 5.

abundant Majorana DM lighter than few tens of GeV, in agreement with [26]. Considering that the lepton number symmetry was spontaneously broken at some scale between 100-2000 GeV, the singlet scalar mass from 0.1-2000 GeV and a mixing angle ensuring $|\cos(\alpha)| > 0.84$, we can have a Majorana fermion as a DM candidate for masses from 30 GeV to 2 TeV. There is a clear resonance due to the Higgs exchange, at $M_N \sim 62.5$ GeV, but if it is going to reach the observed relic density depends mainly on the mixing angle value. Stronger the scalar mixing, more intense the annihilation in standard particles and consequently smaller the relic density for a Majorana fermion at such mass scale. In the limit of null mixing, the relic density is set by annihilations into dark particles and we have found a similar distribution of points, except by the fact that there is no Higgs resonance. This limiting case means that there is no Higgs portal, and thus the dark matter should not be directly observed by non-gravitational interactions. In figure 6 we show two particular values of M_S that set different singlet scalar resonances, for $v_\sigma = 2$ TeV.

Let us now see how the lepton number symmetry breaking scale, v_σ, changes the relic density. In figure 7, we see that there is a global increase in the relic density according to the increase of v_σ, due mainly to the interaction of the Majorana fermion with H, S and J, which is inversely proportional to v_σ (see appendix A). In view of this, we have an upper and a lower allowed scale for the global symmetry breaking to occur in this DM scenario. The plots in figure 7 comprehend all the M_S values, then all the singlet scalar resonances. As we are taking M_S up to 2 TeV, the resonances due to their productions go up to 1 TeV.

We can now look at the parameter space under the light of direct detection experiments.

3.2 Direct detection

The interaction between the Majorana fermion and the quarks is realized via t-channel scalar exchanges. Thus, the scattering cross section is always spin-independent (SI) and in the low energy limit is given by

$$\sigma_{NNqq} \approx \frac{1}{\pi s}\left(\frac{s_\alpha c_\alpha}{v_\sigma v_\phi}\right)^2 \left(\frac{M_N M_q}{M_S M_H}\right)^4 (M_S^2 - M_H^2)^2, \tag{3.3}$$

JHEP09(2015)147

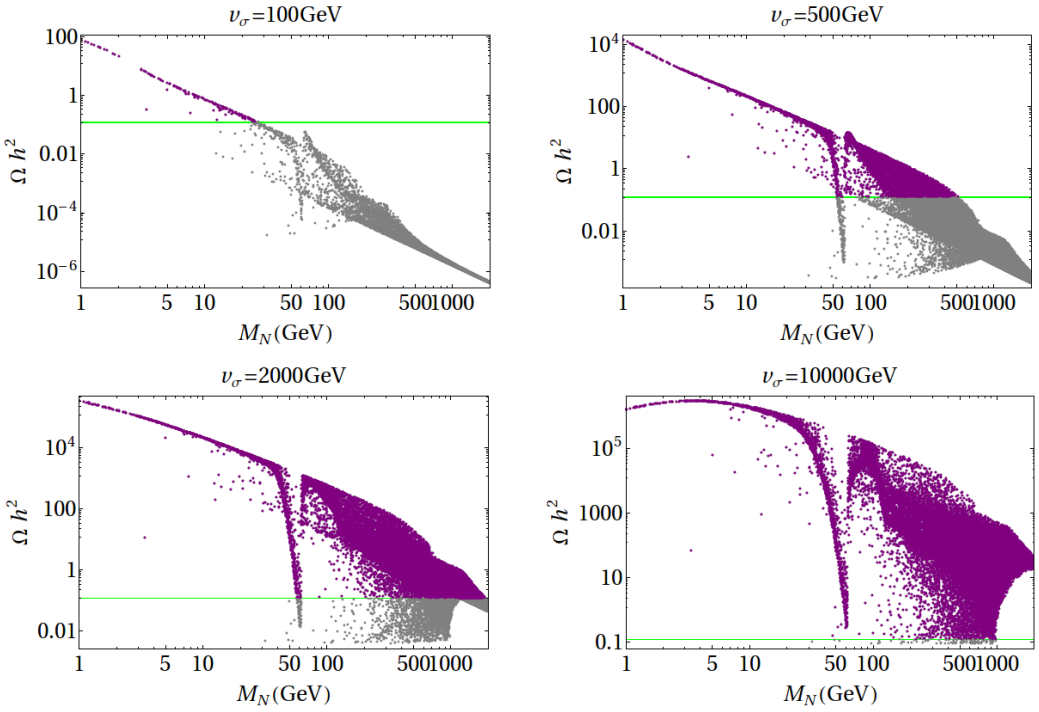

Figure 7. Influence of the lepton number symmetry breaking scale on the relic density. Same color code of figure 5.

where M_q is the quark mass and s is the center of momentum energy. In appendix A we give the general expression for the scattering amplitude of Majorana and standard fermions.

We present a scatter plot for the scattering cross section off nucleon in figure 8, that shows the well known interference effect in the amplitude near the Higgs mass value, as can be expected from eq. (3.3), due to the minus sign coming from the diagonalization of the scalars' mass matrix (eq. (2.9)). This is why the case of $M_S \sim$125 GeV evades the LUX constraint, as well as the future sensitivity of XENON1T, for all the free parameters values considered. We also see the enhancement of the scattering cross section provided by low scalar masses.

In figure 9 we show some plots that clarify the effects of the singlet scalar mass on the WIMP-nucleon scattering cross section, taking into account the points that are excluded by LUX (cyan), that will be accessed by XENON1T (blue) and that are within the Planck interval (green).

The possibility of a lighter than Higgs scalar is still an open question, subjected to a dedicated collider search. The phenomenology and parametrization for light scalars can be found in refs. [38, 39]. Although there exists this possibility in our DM scenario, it is disfavored by the LUX constraint (figure 9, left). Henceforth, we will focus on the case of a singlet scalar heavier than the Higgs boson. As we have already remarked, the case in which the scalars are quite degenerate leads to a cancellation effect in the scattering amplitude, evading direct detection search (figure 9, middle). Notice that XENON1T will be restrictive even for a TeV scale singlet scalar (figure 9, right).

JHEP09(2015)147

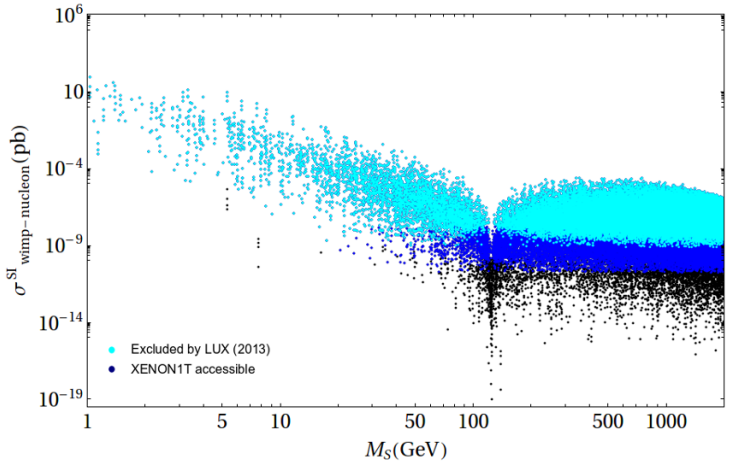

Figure 8. Scattering cross section off nucleon as a function of the singlet scalar mass. The cyan points are already excluded by the LUX results. The blue points are within the XENON1T sensibility. Notice that the case of degenerate scalars can evade the direct detection search for all the free parameters values and very light singlet scalars are not favored since they enhance the scattering cross section.

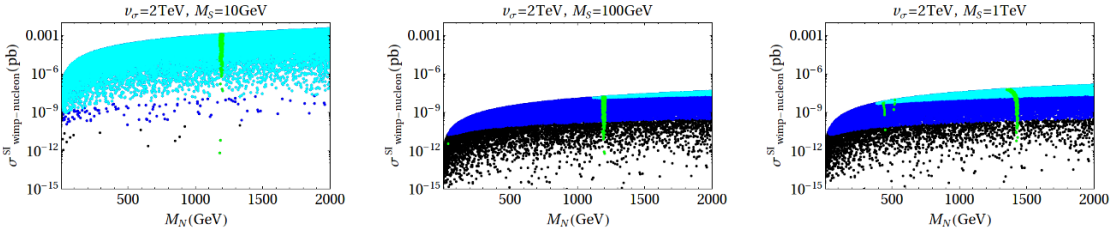

Figure 9. Scattering cross section as a function of the Majorana fermion mass for all values of the mixing angle and certain values of the singlet scalar mass. We see that a lighter than Higgs singlet scalar is disfavored by LUX (left). The cases of a quite degenerate (middle) and a TeV scale (right) singlet scalar can evade the direct detection search, but will be strongly constrained by the XENON1T results. Same color code of the previous figures.

The scalar S is the only new unstable particle of our model, thus it is safe to be sure that its lifetime is smaller than $1s$ in order to agree with big bang nucleosynthesis [40]. For the free parameters intervals considered here, we have found that the S lifetime is between $10^{-28}s$ ($M_S = 2\,\text{TeV}$) and $10^{-13}s$ ($M_S = 100\,\text{MeV}$). Also, the Higgs lifetime that in the SM is predicted to be of the order of $10^{-22}s$ (here for $\alpha = 0$) can be of the order of $10^{-24}s$ (for $|\alpha| = 0.5735$).

The inviability of very light singlet scalars in this model has an interesting consequence. As we have seen, there exists in our spectrum a Majoron, J, that is a massless pseudoscalar. Cosmologically, this particle will naturally contribute to the radiation energy density as long as its interactions keep it coupled to the thermal bath. The last results of Planck satellite are compatible with no extra radiation degrees of freedom [28], although some room for it there still exists. In view of this, it is appropriate to say something concerning the Majoron J in our dark matter scenario.

JHEP09(2015)147

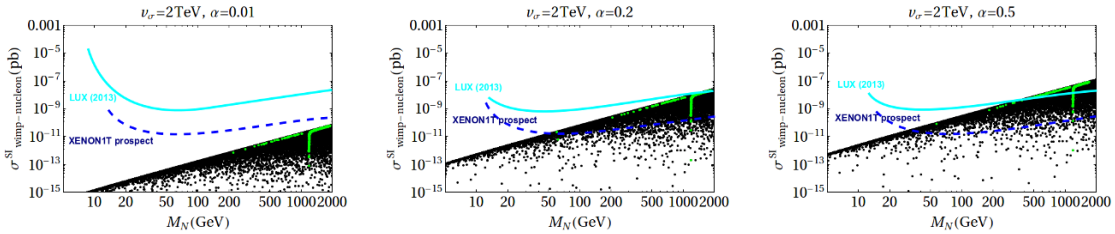

Figure 10. WIMP-nuclen scattering cross section as a function of the Majorana fermion mass for certain values of mixing angle and $M_S > 125\,\text{GeV}$.

The Majoron can be a radiation at the recombination epoch if it decouples just before the muon annihilation [41] and in that case, roughly speaking, we must have

$$\frac{M_S}{\sqrt{|\lambda_{\phi\sigma}|}} \sim 10\,\text{GeV}. \tag{3.4}$$

As we are taking only perturbative mixing coupling values, $\lambda_{\phi\sigma} < 4\pi$ implies that $M_S \lesssim 35\,\text{GeV}$. As we will not consider such a light scalar here, our Majoron will not be regarded as dark radiation.

There is another question concerning our restriction to heavier than Higgs singlet scalars. It is well known that the collisionless cold dark matter (CCDM) paradigm at small scales undergoes tensions by comparing simulation results with observations, but this issue is still far from clear. Small scale structure anomalies, such as core profiles observed in dwarf galaxies and not expected by CCDM-only simulations, suggest that the DM particles may interact significantly with each other [42]. In such self-interacting dark matter context, singlet scalars that open Higgs portals to the dark sector must be light (1–100 MeV) [43, 44]. As we are focusing on heavier singlet scalars in this work, our Majorana fermion is supposed to be in the collisionless regime.

Finally, in figure 10 we see that we can evade the direct detection search for a small enough mixing angle (left), as the interaction of the Majorana fermion with the standard particles is driven by a Higgs portal. This was also observed in ref. [20]. Again, in the scalar degenerate case, when $M_S \sim 125\,\text{GeV}$, we can also evade the direct detection search, but the XENON1T future results should constrain strongly this case as well. In these plots, this case has Planck-allowed points at $M_N \approx 1.2\,\text{TeV}$.

In summary, we have restricted our parameter space by considering only coupling constants within the perturbative regime and ensuring a potential bounded from below. We have considered mixing angles compatible with the maximum mixing allowed for the discovered Higgs boson and examined the impact of the future measurements of the Higgs self-couplings on our model. The values for v_σ were limited from hundreds of GeV to few TeV in order to furnish the observed relic density and we have seen that the existence of a very light singlet scalar is disfavored if we consider it related to the dark matter physics, regarding direct detection. All this analysis is a fair update concerning the issue of DM relic density and direct detection. Once we have a lot of information since the Higgs boson discovery we can use it to further improve our results on the parameter space siege for this model, the so called collider complementarity. We perform this task in the following section.

JHEP09(2015)147

4 Complementarity bounds

This model predicts new decay channels for the Higgs boson, that are so far invisible for the LHC. The new decay rates are given by:

- $\Gamma(H \to JJ) = \frac{M_H^3 s_\alpha^2}{32\pi v_\sigma^2}$;
- $\Gamma(H \to NN) = \frac{1}{16\pi}\frac{s_\alpha^2 M_N^2 M_H}{v_\sigma^2}\left(1 - \frac{4M_N^2}{M_H^2}\right)^{3/2}$;
- $\Gamma(H \to SS) = \frac{M_H^3}{32\pi}\frac{s_\alpha^2 c_\alpha^2}{v_\sigma^2}\left(1 + \frac{2M_S^2}{M_H^2}\right)^2\left(c_\alpha + s_\alpha\frac{v_\sigma}{v_\phi}\right)^2\sqrt{1 - \frac{4M_S^2}{M_H^2}}$.

The upper bound on the branching ratio for invisible Higgs decays (IHD),

$$BR_{\rm inv} = \frac{\Gamma^{\rm inv}}{c_\alpha^2\Gamma^{SM} + \Gamma^{\rm inv}}, \tag{4.1}$$

is $BR_{\rm inv} < 0.34$ in the more general case of floating tree-level couplings to SM particles and $BR_{\rm inv} < 0.22$ if we do not expect new physics in Higgs interactions with photons and gluons [45]. Considering the Higgs decay rate in SM as $\Gamma^{SM} = 4.1\,\text{MeV}$, for the limit of 0.34 (0.22) we have the following general constraint:

$$\frac{\Gamma^{\rm inv}}{c_\alpha^2} < 2.11\ (1.16) \times 10^{-3} GeV. \tag{4.2}$$

As we focus on the case of a heavier than Higgs singlet scalar, there are only two possible hierarchies: $M_H < 2M_S, 2M_N$ and $2M_N < M_H < 2M_S$.

For $\Gamma^{\rm inv} = \Gamma(H \to JJ)$, we have

$$\frac{tg_\alpha^2}{v_\sigma^2} < 1.09 \times 10^{-7}\ (5.95 \times 10^{-8})\ GeV^{-2} \tag{4.3}$$

and for $\Gamma^{\rm inv} = \Gamma(H \to JJ) + \Gamma(H \to NN)$,

$$\frac{tg_\alpha^2}{v_\sigma^2}\left[1 + 2\frac{M_N^2}{M_H^2}\left(1 - \frac{4M_N^2}{M_H^2}\right)^{3/2}\right] < 1.09 \times 10^{-7}\ (5.95 \times 10^{-8})\ GeV^{-2}. \tag{4.4}$$

The translation of the IHD bound to the WIMP-nucleon scattering cross section is often given from the effective field theory point of view. It can be done directly by observing that the interaction between DM and quarks (σ_{SI}) is governed by the same coupling governing the interaction between DM and Higgs ($\Gamma(H \to\ inv)$), both being proportional to the square of the unknown coupling in EFT frameworks (see for example [46]). Therefore, the ratio $\mu \equiv \frac{\sigma_{SI}}{\Gamma(H \to\ inv)} = \frac{\sigma_{SI}}{\Gamma(H \to\ NN)}$ depends only on the DM mass. The IHD bound and its relation with the scattering cross section are given by:

$$BR_{\rm inv} = \frac{(\Gamma(H \to NN))_{EFT}}{\Gamma^{SM} + (\Gamma(H \to NN))_{EFT}} = \frac{(\sigma_{SI})_{EFT}}{\mu(M_N)\Gamma^{SM} + (\sigma_{SI})_{EFT}}. \tag{4.5}$$

JHEP09(2015)147

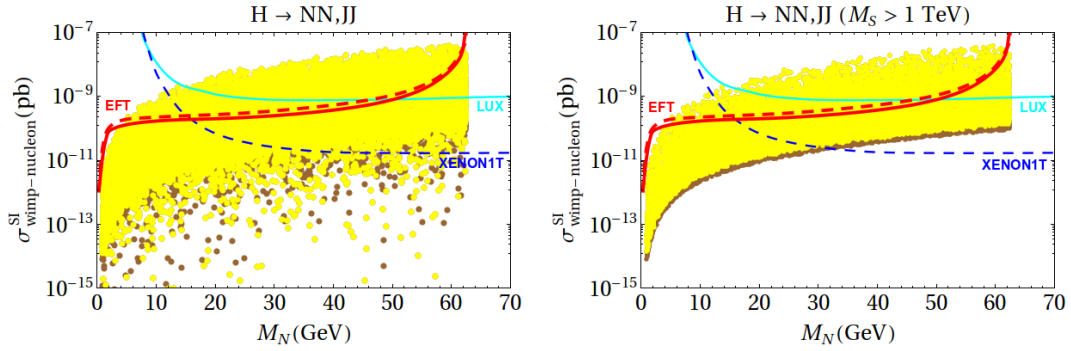

Figure 11. IHD bound on the WIMP-nucleon scattering cross section. The red dashed (solid) line is the effective bound and the yellow (brown) points are excluded in our model for a bound of $BR_{\rm inv} < 0.34$ (0.22). Notice that including Higgs decay into Majorons makes the bound stronger.

This is why in the EFT framework we have upper bound on the WIMP-nucleon scattering cross section coming from the IHD bound, as a function of the WIMP mass:

$$(\sigma_{SI})_{EFT} = \frac{BR_{\rm inv}}{1 - BR_{\rm inv}} \Gamma^{SM} \mu(M_N). \tag{4.6}$$

In our renormalizable model of a fermionic DM, the ratio $\mu = \frac{\sigma_{SI}}{\Gamma(H \to NN,JJ)}$ is smaller than the EFT one because of the Majoron contribution to the Higgs decay and is also a function of M_S and α. Another factor contributing to a stronger upper bound comes from the rescaling of all the Higgs decay rates by c_α^2. The upper bound on the WIMP-nucleon scattering in our scenario is given by

$$\sigma_{SI} = \frac{BR_{\rm inv}}{1 - BR_{\rm inv}} c_\alpha^2 \Gamma^{SM} \mu(M_N, M_S, \alpha). \tag{4.7}$$

As a result, we have an upper bound depending simply on the dark matter mass only in the limit of large M_S and small α.[4] The limitations of the EFT approach for fermionic DM candidates in Higgs Portal models, concerning the LHC and LUX constraints, were considered in refs. [47, 48].

In figure 11, we show in the (M_N, σ^{SI}) plane the upper limits from the IHD bounds within an EFT framework (red lines), extracted from [45]. Dashed (solid) red lines correspond to $BR_{\rm inv} < 0.34$ ($BR_{\rm inv} < 0.22$). Yellow (brown) points are excluded in our model because do not obey equation (4.4). These scans were generated for $M_N < 70\,\text{GeV}$, while α and v_σ are in the ranges of table 1. The left panel shows the excluded points considering M_S from 0.1 GeV to 2 TeV and the right panel shows the excluded points considering $M_S > 1\,\text{TeV}$. Notice that in the latter case the upper bound depends quite exclusively on the WIMP mass. The direct detection bound (cyan line) and prospect (blue line) are also displayed.

As the Z boson do not decay at tree level in singlet scalars in this model, the constraints from invisible Z decay are not relevant here.

[4] In this limit, we recover the EFT bound when the Higgs boson decays exclusively into Majorana fermions.

JHEP09(2015)147

In order to explore the regions of our parameter space allowed by the Planck, LUX and IHD results and accessible by XENON1T detector, we will choose values of the free parameters based on the study of the previous section, instead of arbitrary ones. We do this next by fixing first pairs of free parameters that characterize our scalar sector extension, v_σ and α, and then pairs of mass values of the new particles of our spectrum, M_N and M_S.

For all the following free parameters choices, we have checked that the coupling constant λ_N is always smaller than unity. Also, we have always found viable regions consistent with $|\lambda_{\phi\sigma}| < 1$ for the scans of section 4.1 while all the viable regions in section 4.2 are consistent with it because of LUX results. Contrary to the EFT approach to a Majorana fermion DM [25], that had excluded Higgs-DM coupling strength larger than 10^{-3} in view of XENON100 results, in our renormalizable framework this strength ($\lambda_{NNH} = s_\alpha M_N/v_\sigma$) was found allowed by LUX in the range $10^{-4} - 10^{-1}$.

In what follows, we will identify the regions excluded by the invisible Higgs decay bounds. In figures 12 and 13, the regions filled with yellow (brown) straight lines consist of points that do not obey equations (4.3) or (4.4), being in disagreement with the IHD bounds of $BR_{\rm inv} < 0.34$ $(BR_{\rm inv} < 0.22)$. Consistently with our previous figures, the green lines are composed of points within the Planck interval, while the gray regions are composed of points below the Planck interval, indicating the regions of the parameter space in which the Majorana fermion could be only a fraction of the total DM content of the Universe. Although we do not consider another DM candidate or non-thermal production that validate these gray points, we keep it for completeness. Regarding the direct detection search, the cyan regions are excluded by LUX and the dashed blue lines will extend this exclusion if XENON1T do not confirm any DM signal in a close future.

4.1 v_σ and α fixed

In this subsection, we fix a set of values for the new vev, v_σ, and the mixing angle, α, that parametrize the scalar extension of this model. Based on our previous results, illustrated by figure 7, we will study how the lepton number breaking scale changes the allowed regions by choosing $v_\sigma = 500\,\text{GeV}$, 1 TeV and 2 TeV. The role of the mixing angle is considered by taking it as $\alpha = 0.01$, 0.2 and 0.5.

In figure 12, we display the free parameter slice (M_N, M_S) for different pairs of α and v_σ. All the Planck-allowed points (green) are near the scalar resonance, in agreement with previous works. For strong enough scalar mixing ($\alpha = 0.2$ and $\alpha = 0.5$ in this figure) we see Planck-allowed points for $M_N \sim M_H/2 = 62.5\,\text{GeV}$, corresponding to the Higgs resonance. As we are varying M_S up to 2 TeV, in the three first plots (for $v_\sigma = 2\,\text{TeV}$) the Planck-allowed points for $M_N < 1\,\text{TeV}$ correspond to the singlet scalar resonances and the ones for $M_N > 1\,\text{TeV}$, to the dips of the abundance curve (see figure 6).

The IHD constraints are able to exclude all the Planck-allowed points in two extremes: higher α value (right upper panel), excluded only by the stronger IHD bound, and lower v_σ value (left lower panel), excluded by the two IHD bounds. Note that these two extremes correspond to higher deviations from the standard scalar sector and are currently disfavored by LHC physics. For $\alpha = 0.01$ and $\alpha = 0.2$ with $v_\sigma = 2\,\text{TeV}$, the direct detection search do not exclude any Planck-allowed point, but for $\alpha = 0.5$ it offers a strong limit. We see that

JHEP09(2015)147

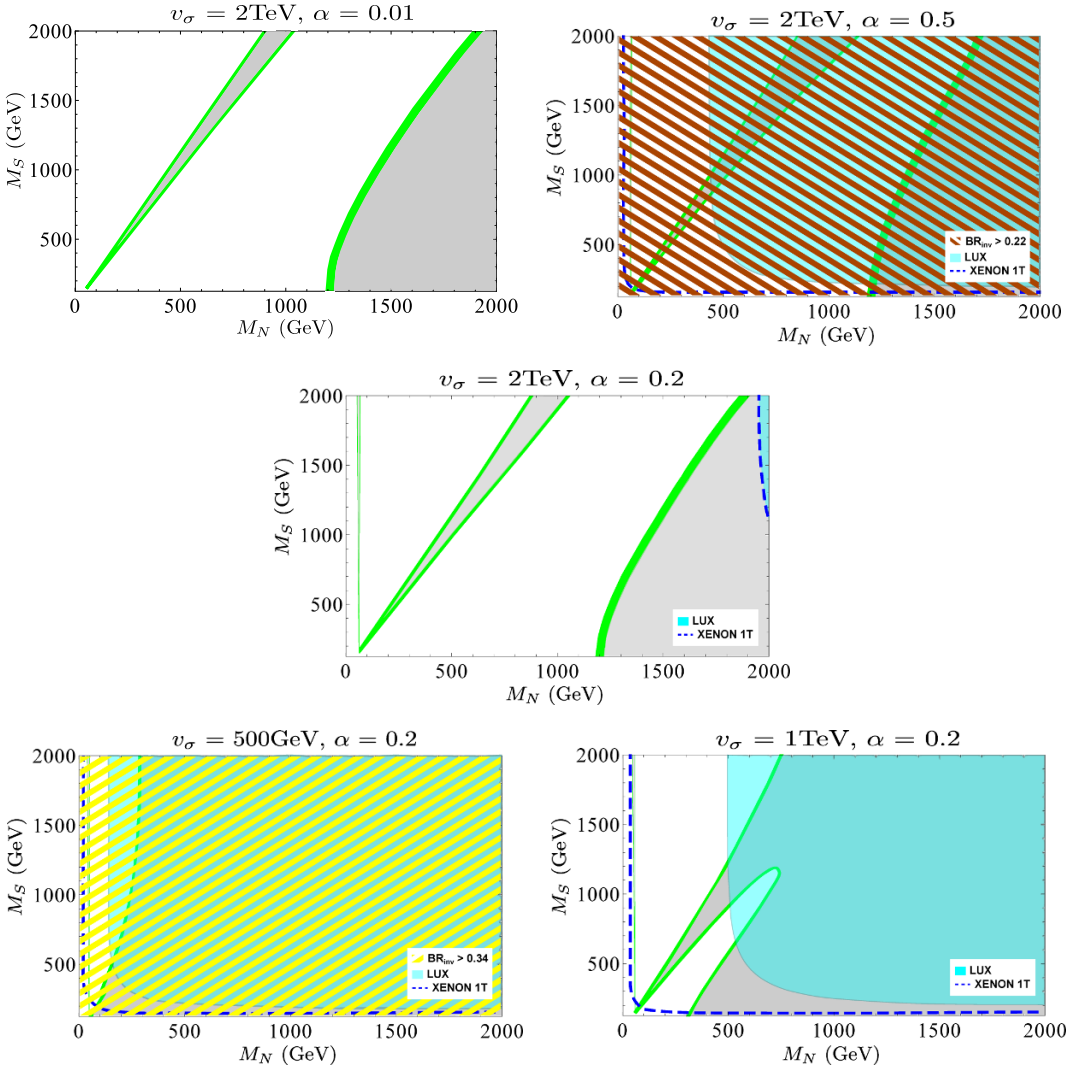

Figure 12. Free parameter slices (M_N, M_S) for fixed v_σ values (upper panel) and fixed α values (lower panel). The green regions are in agreement with Planck 2015 results while the gray ones provide underabundant Majorana fermion. The cyan regions are already excluded by LUX and the blue dashed lines show the XENON1T sensitivity limit that could expand the LUX exclusion (or point out dark matter new physics, of course). The yellow (brown) straight lines show the regions excluded by IHD into two Majorons or two Majorons and two Majorana fermions for the upper bound of 0.34 (0.22).

$M_N > 500\,\text{GeV}$ is excluded by LUX for $\alpha = 0.5$ if $M_S > 500\,\text{GeV}$ and will be completely probed by XENON1T. For a $v_\sigma = 1$ TeV (right lower panel), we see that $M_N > 500\,\text{GeV}$ is also excluded by LUX for $\alpha = 0.2$ if $M_S > 500\,\text{GeV}$ but in comparison with the case "$v_\sigma = 2\,\text{TeV}$, $\alpha = 0.5$" (right upper panel), we have more Planck-allowed points in the LUX-allowed region.

In the limit of null mixing ($\alpha \to 0$) and very high energy breaking scale of the symmetry we are supposing ($v_\sigma \to \infty$), the scalar sector of our model becomes standard, with just one

JHEP09(2015)147

scalar coming from a doublet, no Majoron in the spectrum and without the possibility of providing mass for our dark matter candidate. As we have seen in figure 12, our parameter space is favored by small deviations of the scalar sector, it means, for smaller scalar mixing and high lepton number breaking scale (few TeV, left upper panel), in view of the current collider and direct detection searches. We have seen that the model we consider here is very predictive and in the next few years, all this scenario should be tested by the experiments. It is constructive to keep in mind, however, that the confirmation of a possible DM particle signal *and* a possible discovery of a new scalar at colliders are closely related things in Higgs portal models and their immersion in more complex contexts may offer important hints.

4.2 M_N and M_S fixed

Now we study the allowed parameter space for fixed values of M_N and M_S. Here we consider the lepton number breaking scale, v_σ, in a larger window, from 100 GeV to 10 TeV. The TeV scale is a natural scale in the search for new physics, then we study separately the case of $M_N = 1\,\text{TeV}$ and $M_S = 1\,\text{TeV}$. For a $M_N = 1\,\text{TeV}$, we show how the allowed region depends on M_S by fixing it at 130 GeV (quite degenerate case), 500 GeV (intermediate case) and 1 TeV (TeV scale physics). On the other hand, for $M_S = 1\,\text{TeV}$, we consider Majorana fermions with masses of 60 GeV (Higgs resonance case) and 500 GeV (singlet scalar resonance case).

In figure 13, we show the free parameter slices (α, v_σ). In the upper and middle panels, we have the case of $M_N = 1\,\text{TeV}$. The Majorana fermion might be sufficiently abundant only if v_σ is near 2 TeV, regardless the singlet scalar mass, implying that its interaction with the scalars would be weak (see eq. (2.15)). Lower breaking scales would need another DM candidate or a non-thermal DM production, to be constrained by IHD, LUX and XENON1T. As we already pointed out, the quite degenerate case (left upper panel) can evade direct detection. The Higgs data provide the strongest current bound, allowing for scalar mixing up to 0.4. For heavier singlet scalars, the current limits for the mixing are $\alpha \lesssim 0.3$ for $M_S = 500\,\text{GeV}$ (right upper panel) and $\alpha \lesssim 0.25$ for $M_S = 1\,\text{TeV}$ (middle panel). The XENON1T future limits might restrict much more the mixing, up to $\alpha \lesssim 0.05$, in which case non-standard interactions will not be detected easily.

In the lower panel, we can appreciate how the scalar resonance regions of the spectrum evade the current experimental bounds. At left, we show the Higgs resonance case ($M_N = 60\,\text{GeV}$), where the LHC bound is stronger than LUX bound but cannot constrain a sufficiently abundant Majorana fermion. In this case, the breaking scale should be from 200 GeV (for small mixing) to 5 TeV (for maximal mixing). Nevertheless, it will be completely probed in the next few years by XENON1T. At right, we show the singlet scalar resonance ($M_N = 500\,\text{GeV}$), also not constrained by the current bounds but accessible to XENON1T, when the mixing might become restricted to $\alpha \lesssim 0.1$. This possibility requires the breaking scale near 5 TeV for a sufficiently abundant Majorana fermion.

We have seen that even the safer resonance regions might be strongly constrained in the near future, and even considering a TeV scale new physics.

JHEP09(2015)147

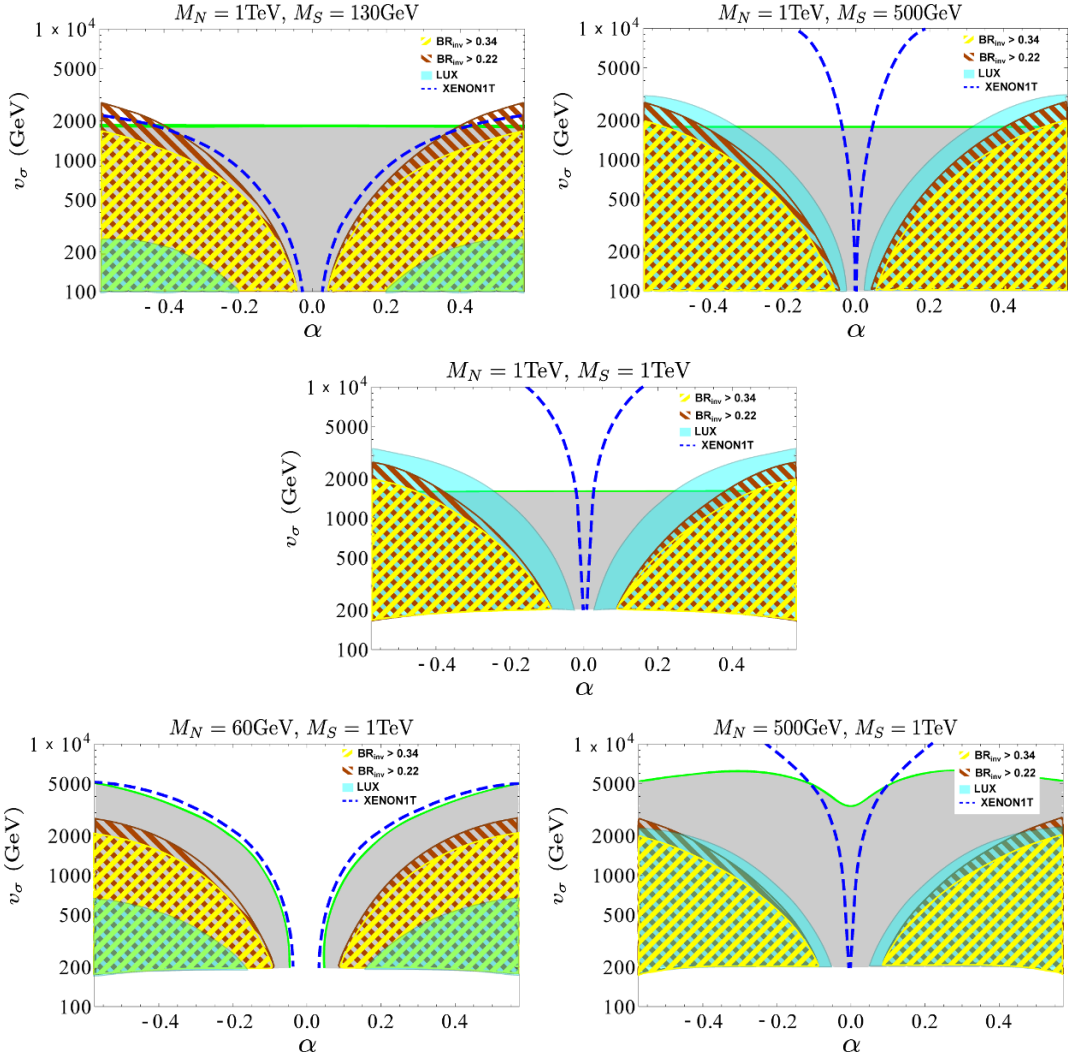

Figure 13. Free parameter slices (α, v_σ) for fixed M_N values (upper panel) and fixed M_S values (lower panel). Same color code of figure 12.

5 Conclusions

In this work we updated a CP-conserving Higgs portal model of a Majorana fermion dark matter, opened by a complex singlet scalar, in view of the latest Planck, LUX and invisible Higgs decay (IHD) constraints and the XENON1T prospects. This model is described by only four parameters: the Majorana fermion and singlet scalar masses, M_N and M_S, the mixing angle between the scalars, α, and a lepton number breaking scale, v_σ.

Our parameter space is within the sensibility of the future collider searches in what concerns to the 3-Higgs self-coupling constant. It means that the measurement of the Higgs self-coupling can shed light on our Majorana fermion DM scenario. Also, strong deviations from the SM value of the 4-Higgs self-coupling could set the scalar hierarchy, providing important hints for future scalar searches. All the analysis we have made is within the perturbative regime and is compatible with a bounded from below scalar potential.

JHEP09(2015)147

We found that v_σ must be between few hundreds of GeV and few TeV in order to the Majorana fermion account for the total amount of DM in the Universe, according to the Planck results. Considering that this symmetry breaking took place at some scale between 100-2000 GeV, the singlet scalar mass from 0.1-2000 GeV and a mixing angle ensuring $|\cos(\alpha)| > 0.84$, we can have a Majorana fermion as a DM candidate for masses from 30 GeV to 2 TeV. The case of a lighter than Higgs singlet scalar in this DM scenario is very disfavored by LUX, which also guarantees that the Majoron is not an extra radiation component, in agreement with Planck results [28].

With the aim of splitting the degeneracy of this allowed region, we studied the role of each parameter to find the very predictive curves allowed by Planck and contrasted by the experimental limits. We did it systematically by choosing benchmark values for pairs of free parameters characterizing the scalar sector extension (α and v_σ) and the mass spectrum (M_N and M_S). As expected, the allowed regions are near the scalar resonances. We have shown that it is possible to evade the LUX and even the future XENON1T constraints for a Majorana DM candidate in two situations: scalar degenerate case (figure 9) and small mixing angles (figure 10).

Considering the 'universal Higgs fit' [45], the IHD bound for free tree-level Higgs couplings to standard particles ($BR_{\text{inv}} < 0.34$) excludes a hundred-GeV lepton breaking scale ($v_\sigma = 500\,\text{GeV}$) and the IHD bound that do not allow for new physics at loop Higgs couplings to gluons and photons ($BR_{\text{inv}} < 0.22$) excludes the maximal mixing case ($\alpha = 0.5$) as well. It means that the LHC data disfavors large deviations from the standard scalar sector in our dark matter scenario. TeV scale v_σ values were found safe (figure 12). We have shown that $M_N > 500\,\text{GeV}$ is excluded by LUX if $M_S > 500\,\text{GeV}$ in the case "$v_\sigma = 1\,\text{TeV}$,$\alpha = 0.2$" (right upper and lower of figure 12).

For $M_N = 1\,\text{TeV}$, v_σ must be at approximately 2 TeV in order to agree with the Planck results and the mixing was found restricted to $\alpha \lesssim 0.3$ (for $M_S = 500\,\text{GeV}$) and $\alpha \lesssim 0.25$ (for $M_S = 1\,\text{TeV}$) by the LUX results and to $\alpha \lesssim 0.05$ by the XENON1T future bound (upper and middle panels of figure 13). It means that if no signal is confirmed by XENON1T, it becomes very difficult to detect some non-standard interaction at colliders, since they should be proportional to $\sin(\alpha)^2$. The resonance regions were found not constrained by the current experiments, but XENON1T might exclude completely $M_N \sim 60\,\text{GeV}$ and restrict the mixing to $\alpha \lesssim 0.1$ for $M_S = 1\,\text{TeV}$ (lower panel of figure 13).

All the analysis we have made shows how "narrow" the Higgs portal we consider here is, in the sense that the current experimental bounds are very restrictive for large deviations of the SM scalar sector in our dark matter model. We have seen how the discoveries of a DM and a new scalar particles are strongly related in our Higgs portal scenario (figure 12). While this minimal scheme remains allowed by the experimental bounds, it can be embedded in more fundamental extensions of the SM. In supersymmetric theories, stable neutralinos are Majorana fermions that also appear as natural dark matter candidates and in some gauge extensions where neutral scalars may be the remnants of a more fundamental gauge symmetry breaking, as studied in [49].

JHEP09(2015)147

A Amplitudes for Majorana fermion annihilation processes

Here we present the amplitudes for the Majorana fermion annihilation processes shown in figure 4. Note that in the limit of null scalar mixing, there is no interaction between the visible and dark sectors. Hereafter, the initial momenta are denoted by p_1 and p_2, the final momenta by p_1' and p_2' and the momenta of virtual particles i by k_i.

- Majorana fermion annihilation into SM particles:

$$\begin{aligned}\mathcal{M}(NN \to HH) = & -i\bar{v}(p_1)\left\{\left(6s_\alpha\lambda_{HHH}\frac{M_N}{v_\sigma}\right)\frac{1}{k_H^2-M_H^2}\right.\\ & +\left(2c_\alpha\lambda_{SHH}\frac{M_N}{v_\sigma}\right)\frac{1}{k_S^2-M_S^2}\\ & \left.+\left(s_\alpha\frac{M_N}{v_\sigma}\right)^2\frac{\not{k}_N+M_N}{k_N^2-M_N^2}\right\}u(p_2); \qquad \text{(A.1)}\end{aligned}$$

$$\begin{aligned}\mathcal{M}(NN \to ff) = & -i\left(s_\alpha c_\alpha\frac{M_N M_f}{v_\sigma v_\phi}\right)\times\\ & \times\left(\frac{1}{k_H^2-M_H^2}-\frac{1}{k_S^2-M_S^2}\right)\bar{v}(p_1)u(p_2)\bar{u}(p_1')v(p_2'); \qquad \text{(A.2)}\end{aligned}$$

$$\mathcal{M}(NN \to VV) = i\left(s_\alpha c_\alpha\lambda_{hVV}\frac{M_N}{v_\sigma}\right)\left(\frac{1}{k_H^2-M_H^2}-\frac{1}{k_S^2-M_S^2}\right)\bar{v}(p_1)u(p_2); \qquad \text{(A.3)}$$

  where f stands for fermions and V for the vector bosons and

$$\lambda_{hVV} = 2M_V^2(G_F\sqrt{2})^{1/2} \qquad \text{(A.4)}$$

$$\lambda_{SHH} = \frac{s_\alpha c_\alpha}{2v_\phi v_\sigma}(v_\phi s_\alpha - v_\sigma c_\alpha)(2M_H^2+M_S^2). \qquad \text{(A.5)}$$

- Amplitudes for annihilation into dark particles:

$$\begin{aligned}\mathcal{M}(NN \to SS) = & -i\bar{v}(p_1)\left\{\left(2s_\alpha\lambda_{HSS}\frac{M_N}{v_\sigma}\right)\frac{1}{k_H^2-M_H^2}\right.\\ & +\left(6c_\alpha\lambda_{SSS}\frac{M_N}{v_\sigma}\right)\frac{1}{k_S^2-M_S^2}\\ & \left.+\left(c_\alpha\frac{M_N}{v_\sigma}\right)^2\frac{\not{k}_N+M_N}{k_N^2-M_N^2}\right\}u(p_2); \qquad \text{(A.6)}\end{aligned}$$

$$\begin{aligned}\mathcal{M}(NN \to JJ) = & -i\bar{v}(p_1)\left\{\left(s_\alpha^2\frac{M_N M_H^2}{v_\sigma^2}\right)\frac{1}{k_H^2-M_H^2}\right.\\ & +\left(c_\alpha^2\frac{M_N M_S^2}{v_\sigma^2}\right)\frac{1}{k_S^2-M_S^2}\\ & \left.+\left(\frac{M_N}{v_\sigma}\right)^2\frac{\not{k}_N+M_N}{k_N^2-M_N^2}\right\}u(p_2); \qquad \text{(A.7)}\end{aligned}$$

$$\mathcal{M}(NN \to HJ) = \bar{v}(p_1)\gamma_5\left\{\left(s_\alpha\frac{M_N M_H^2}{v_\sigma^2}\right)\frac{1}{k_J^2}+\left(s_\alpha\frac{M_N^2}{v_\sigma^2}\right)\frac{\not{k}_N+M_N}{k_N^2-M_N^2}\right\}u(p_2); \qquad \text{(A.8)}$$

JHEP09(2015)147

$$\mathcal{M}(NN \to SJ) = \bar{v}(p_1)\gamma_5 \left\{ \left(c_\alpha \frac{M_N M_S^2}{v_\sigma^2} \right) \frac{1}{k_J^2} + \left(c_\alpha \frac{M_N^2}{v_\sigma^2} \right) \frac{\not{k}_N + M_N}{k_N^2 - M_N^2} \right\} u(p_2); \quad \text{(A.9)}$$

$$\begin{aligned} \mathcal{M}(NN \to HS) = & -i\bar{v}(p_1) \Bigg\{ \left(2 s_\alpha \lambda_{SHH} \frac{M_N}{v_\sigma} \right) \frac{1}{k_H^2 - M_H^2} \\ & + \left(2 c_\alpha \lambda_{HSS} \frac{M_N}{v_\sigma} \right) \frac{1}{k_S^2 - M_S^2} \\ & + \left(s_\alpha c_\alpha \frac{M_N^2}{v_\sigma^2} \right) \frac{\not{k}_N + M_N}{k_N^2 - M_N^2} \Bigg\} u(p_2); \end{aligned} \quad \text{(A.10)}$$

where

$$\lambda_{HSS} = \frac{s_\alpha c_\alpha}{2 v_\phi v_\sigma} (v_\phi c_\alpha + v_\sigma s_\alpha)(2 M_S^2 + M_H^2); \quad \text{(A.11)}$$

$$\lambda_{SSS} = \frac{M_S^2}{2 v_\sigma} \left(c_\alpha^3 - s_\alpha^3 \frac{v_\sigma}{v_\phi} \right). \quad \text{(A.12)}$$

In the limit of null scalar mixing, $\alpha = 0$, the amplitudes leading to a relic density of dark matter are:

$$\mathcal{M}(NN \to SS) \to -i\bar{v}(p_1) \left\{ \left(\frac{3 M_N M_S^2}{2 v_\sigma^2} \right) \frac{1}{k_S^2 - M_S^2} + \left(\frac{M_N}{v_\sigma} \right)^2 \frac{\not{k}_N + M_N}{k_N^2 - M_N^2} \right\} u(p_2); \quad \text{(A.13)}$$

$$\mathcal{M}(NN \to JJ) \to -i\bar{v}(p_1) \left\{ \left(\frac{M_N M_S^2}{v_\sigma^2} \right) \frac{1}{k_S^2 - M_S^2} + \left(\frac{M_N}{v_\sigma} \right)^2 \frac{\not{k}_N + M_N}{k_N^2 - M_N^2} \right\} u(p_2); \quad \text{(A.14)}$$

$$\mathcal{M}(NN \to SJ) \to \bar{v}(p_1)\gamma_5 \left\{ \left(\frac{M_N M_S^2}{v_\sigma^2} \right) \frac{1}{k_J^2} + \left(\frac{M_N}{v_\sigma} \right)^2 \frac{\not{k}_N + M_N}{k_N^2 - M_N^2} \right\} u(p_2). \quad \text{(A.15)}$$

Acknowledgments

We are very grateful to Clarissa Siqueira, Antonio Oliveira and Farinaldo Queiroz for useful discussions. We also thank to Ian Shoemaker for his comments concerning self-interacting dark matter. This work was supported by Coordenação de Aperfeiçoamento de Pessoal de Nível Superior — CAPES (MD) and Conselho Nacional de Desenvolvimento Científico e Tecnológico — CNPq (CASP,PSRS).

References

[1] F. Zwicky, *Republication of: the redshift of extragalactic nebulae*, *Gen. Rel. Grav.* **41** (2009) 207.

JHEP09(2015)147

[2] V.C. Rubin and W.K. Ford, Jr., *Rotation of the andromeda nebula from a spectroscopic survey of emission regions*, *Astrophys. J.* **159** (1970) 379 [INSPIRE].

[3] M.A. Monroy-Rodríguez and C. Allen, *The end of the MACHO era- revisited: new limits on MACHO masses from halo wide binaries*, *Astrophys. J.* **790** (2014) 159 [arXiv:1406.5169] [INSPIRE].

[4] D. Clowe et al., *A direct empirical proof of the existence of dark matter*, *Astrophys. J.* **648** (2006) L109 [astro-ph/0608407] [INSPIRE].

[5] A. Klypin and F. Prada, *Testing gravity with motion of satellites around galaxies: newtonian gravity against Modified Newtonian Dynamics*, *Astrophys. J.* **690** (2009) 1488 [arXiv:0706.3554] [INSPIRE].

[6] S. Dodelson, *The real problem with MOND*, *Int. J. Mod. Phys.* **D 20** (2011) 2749 [arXiv:1112.1320] [INSPIRE].

[7] H. Goldberg and L.J. Hall, *A new candidate for dark matter*, *Phys. Lett.* **B 174** (1986) 151.

[8] A. de Rújula, S.L. Glashow and U. Sarid, *Charged dark matter*, *Nucl. Phys.* **B 333** (1990) 173.

[9] L. Chuzhoy and E.W. Kolb, *Reopening the window on charged dark matter*, *JCAP* **07** (2009) 014 [arXiv:0809.0436] [INSPIRE].

[10] CMS collaboration, *Observation of a new boson at a mass of 125 GeV with the CMS experiment at the LHC*, *Phys. Lett.* **B 716** (2012) 30 [arXiv:1207.7235] [INSPIRE].

[11] ATLAS collaboration, *Observation of a new particle in the search for the standard model Higgs boson with the ATLAS detector at the LHC*, *Phys. Lett.* **B 716** (2012) 1 [arXiv:1207.7214] [INSPIRE].

[12] S. Baek, P. Ko and W.-I. Park, *Search for the Higgs portal to a singlet fermionic dark matter at the LHC*, *JHEP* **02** (2012) 047 [arXiv:1112.1847] [INSPIRE].

[13] M.A. Fedderke, J.-Y. Chen, E.W. Kolb and L.-T. Wang, *The fermionic dark matter Higgs portal: an effective field theory approach*, *JHEP* **08** (2014) 122 [arXiv:1404.2283] [INSPIRE].

[14] L. Lopez-Honorez, T. Schwetz and J. Zupan, *Higgs portal, fermionic dark matter and a Standard Model like Higgs at 125 GeV*, *Phys. Lett.* **B 716** (2012) 179 [arXiv:1203.2064] [INSPIRE].

[15] N. Okada and T. Yamada, *Simple fermionic dark matter models and Higgs boson couplings*, *JHEP* **10** (2013) 017 [arXiv:1304.2962] [INSPIRE].

[16] T. Boeckel and J. Schaffner-Bielich, *Cosmology of fermionic dark matter*, *Phys. Rev.* **D 76** (2007) 103509 [arXiv:0707.3260] [INSPIRE].

[17] K. Ghorbani, *Fermionic dark matter with pseudo-scalar Yukawa interaction*, *JCAP* **01** (2015) 015 [arXiv:1408.4929] [INSPIRE].

[18] Z. Bagherian, M.M. Ettefaghi, Z. Haghgouyan and R. Moazzemi, *A new parameter space study of the fermionic cold dark matter model*, *JCAP* **10** (2014) 033 [arXiv:1406.2927] [INSPIRE].

[19] T.H. Franarin, C.A.Z. Vasconcellos and D. Hadjimichef, *On the possibility of a 130 GeV gamma-ray line from annihilating singlet fermionic dark matter*, *Astron. Nachr.* **335** (2014) 647 [arXiv:1404.0406] [INSPIRE].

JHEP09(2015)147

[20] M. Fairbairn and R. Hogan, *Singlet fermionic dark matter and the electroweak phase transition*, *JHEP* **09** (2013) 022 [arXiv:1305.3452] [INSPIRE].

[21] C.-K. Chua and R.-C. Hsieh, *Study of Dirac fermionic dark matter*, *Phys. Rev.* **D 88** (2013) 036011 [arXiv:1305.7008] [INSPIRE].

[22] Y.G. Kim, K.Y. Lee and S. Shin, *Singlet fermionic dark matter*, *JHEP* **05** (2008) 100 [arXiv:0803.2932] [INSPIRE].

[23] S. Baek, P. Ko, W.-I. Park and E. Senaha, *Vacuum structure and stability of a singlet fermion dark matter model with a singlet scalar messenger*, *JHEP* **11** (2012) 116 [arXiv:1209.4163] [INSPIRE].

[24] S. Esch, M. Klasen and C.E. Yaguna, *Detection prospects of singlet fermionic dark matter*, *Phys. Rev.* **D 88** (2013) 075017 [arXiv:1308.0951] [INSPIRE].

[25] A. Djouadi, O. Lebedev, Y. Mambrini and J. Quevillon, *Implications of LHC searches for Higgs–portal dark matter*, *Phys. Lett.* **B 709** (2012) 65 [arXiv:1112.3299] [INSPIRE].

[26] S. Matsumoto, S. Mukhopadhyay and Y.-L.S. Tsai, *Singlet Majorana fermion dark matter: a comprehensive analysis in effective field theory*, *JHEP* **10** (2014) 155 [arXiv:1407.1859] [INSPIRE].

[27] C.A. de S. Pires, F.S. Queiroz and P.S. Rodrigues da Silva, *Singlet Majorana fermion dark matter, DAMA, CoGeNT and CDMS-II*, *Phys. Rev.* **D 82** (2010) 105014 [arXiv:1002.4601] [INSPIRE].

[28] PLANCK collaboration, P.A.R. Ade et al., *Planck 2015 results. XIII. Cosmological parameters*, arXiv:1502.01589 [INSPIRE].

[29] LUX collaboration, D.S. Akerib et al., *First results from the LUX dark matter experiment at the Sanford Underground Research Facility*, *Phys. Rev. Lett.* **112** (2014) 091303 [arXiv:1310.8214] [INSPIRE].

[30] XENON1T collaboration, E. Aprile, *The XENON1T dark matter search experiment*, *Springer Proc. Phys.* **148** (2013) 93 [arXiv:1206.6288] [INSPIRE].

[31] G. Bélanger, F. Boudjema, A. Pukhov and A. Semenov, *MicrOMEGAs_3: a program for calculating dark matter observables*, *Comput. Phys. Commun.* **185** (2014) 960 [arXiv:1305.0237] [INSPIRE].

[32] D.G.E. Walker, *Unitarity Constraints on Higgs Portals*, arXiv:1310.1083 [INSPIRE].

[33] S. Profumo, M.J. Ramsey-Musolf, C.L. Wainwright and P. Winslow, *Singlet-catalyzed electroweak phase transitions and precision Higgs boson studies*, *Phys. Rev.* **D 91** (2015) 035018 [arXiv:1407.5342] [INSPIRE].

[34] A.J. Barr, M.J. Dolan, C. Englert, D.E. Ferreira de Lima and M. Spannowsky, *Higgs self-coupling measurements at a 100 TeV hadron collider*, *JHEP* **02** (2015) 016 [arXiv:1412.7154] [INSPIRE].

[35] A. Conway, H. Wenzel, R. Lipton and E. Eichten, *Measuring the Higgs self-coupling constant at a multi-TeV muon collider*, arXiv:1405.5910 [INSPIRE].

[36] ILD collaboration, J. Tian and K. Fujii, *Measurement of Higgs couplings and self-coupling at the ILC*, PoS(EPS-HEP 2013)316 [arXiv:1311.6528] [INSPIRE].

[37] F. Goertz, A. Papaefstathiou, L.L. Yang and J. Zurita, *Measuring the Higgs boson self-coupling at the LHC using ratios of cross sections*, arXiv:1309.3805 [INSPIRE].

JHEP09(2015)147

[38] J.D. Clarke, R. Foot and R.R. Volkas, *Phenomenology of a very light scalar (*100 *MeV* $< m_h <$ 10 *GeV) mixing with the SM Higgs*, *JHEP* **02** (2014) 123 [arXiv:1310.8042] [INSPIRE].

[39] G. Cacciapaglia, A. Deandrea, G.D. La Rochelle and J.-B. Flament, *Searching for a lighter Higgs boson: parametrization and sample tests*, *Phys. Rev.* **D 91** (2015) 015012 [arXiv:1311.5132] [INSPIRE].

[40] M. Kaplinghat, S. Tulin and H.-B. Yu, *Direct detection portals for self-interacting dark matter*, *Phys. Rev.* **D 89** (2014) 035009 [arXiv:1310.7945] [INSPIRE].

[41] S. Weinberg, *Goldstone bosons as fractional cosmic neutrinos*, *Phys. Rev. Lett.* **110** (2013) 241301 [arXiv:1305.1971] [INSPIRE].

[42] D.N. Spergel and P.J. Steinhardt, *Observational evidence for selfinteracting cold dark matter*, *Phys. Rev. Lett.* **84** (2000) 3760 [astro-ph/9909386] [INSPIRE].

[43] S. Tulin, H.-B. Yu and K.M. Zurek, *Beyond collisionless dark matter: particle physics dynamics for dark matter halo structure*, *Phys. Rev.* **D 87** (2013) 115007 [arXiv:1302.3898] [INSPIRE].

[44] C. Kouvaris, I.M. Shoemaker and K. Tuominen, *Self-interacting dark matter through the Higgs portal*, *Phys. Rev.* **D 91** (2015) 043519 [arXiv:1411.3730] [INSPIRE].

[45] P.P. Giardino, K. Kannike, I. Masina, M. Raidal and A. Strumia, *The universal Higgs fit*, *JHEP* **05** (2014) 046 [arXiv:1303.3570] [INSPIRE].

[46] A. Djouadi, A. Falkowski, Y. Mambrini and J. Quevillon, *Direct detection of Higgs-portal dark matter at the LHC*, *Eur. Phys. J.* **C 73** (2013) 2455 [arXiv:1205.3169] [INSPIRE].

[47] S. Baek, P. Ko and W.-I. Park, *Invisible Higgs decay width vs. dark matter direct detection cross section in Higgs portal dark matter models*, *Phys. Rev.* **D 90** (2014) 055014 [arXiv:1405.3530] [INSPIRE].

[48] G. Busoni, A. De Simone, E. Morgante and A. Riotto, *On the validity of the effective field theory for dark matter searches at the LHC*, *Phys. Lett.* **B 728** (2014) 412 [arXiv:1307.2253] [INSPIRE].

[49] P.V. Dong, D.T. Huong, F.S. Queiroz and N.T. Thuy, *Phenomenology of the 3-3-1-1 model*, *Phys. Rev.* **D 90** (2014) 075021 [arXiv:1405.2591] [INSPIRE].

JHEP09(2015)147